Image Cover Sheet

CLASSIFICATION	SYSTEM NUMBER	503453
UNCLASSIFIED		

TITLE

HYDRODYNAMIC INTERACTION FORCES BETWEEN TWO SHIPS IN WAVES

System Number:

Patron Number:

Requester:

Notes:

DSIS Use only:

Deliver to:

HYDRODYNAMIC INTERACTION FORCES BETWEEN TWO SHIPS IN WAVES

Y. J. He, Centre for Marine Vessel Design and Research, Faculty of Engineering, Dalhousie University, (formerly Technical University of Nova Scotia), Halifax, Nova Scotia, B3J 2X4
K. McTaggart, Defence Research Establishment Atlantic, P.O. Box 1012, Dartmouth, Nova Scotia, B2Y 3Z7
C. C. Hsiung, Centre for Marine Vessel Design and Research, Faculty of Engineering, Dalhousie University, (formerly Technical University of Nova Scotia), Halifax, Nova Scotia, B3J 2X4

Abstract

The hydrodynamic interaction forces in waves are computed for two ships advancing in parallel at the same speed. The forces considered are due to added mass, wave radiation damping, and wave excitation including diffraction effects. The coupled hydrodynamic forces are computed by the three-dimensional panel method using the zero speed Green function, with extensions to include forward speed effects. The theoretical formulation correctly satisfies boundary conditions on both ship hulls simultaneously. The wave diffraction problem is solved for the presence of both ships in a stationary state. The wave radiation problem is solved by assuming one ship is in motion while the other is at rest. Examples are given for two stationary vertical circular cylinders and for a small vessel advancing in close proximity to a large supply vessel.

NOMENCLATURE

a	wave amplitude
B_b	beam of ship-b
F_j^a	force component j on ship-a
F_j^{Ra}	radiation force component j on ship-a
F_j^{Wa}	wave excitation force component j on ship-a
f_j^{Ia}	complex incident force j on ship-a
f_j^{Da}	complex diffracted force j on ship-a
k	wavenumber
L_b	length of ship-b
m_k^a	generalized normal at speed for mode k of ship-a
n_j^a	normal on ship-a for mode j
p	hydrodynamic pressure or field point
q	source point
R	horizontal distance from field point to source
r	cylinder radius
r_1	distance from field point to source
r_2	distance from field point to image source
$\vec{r}_a$	moment arm vector
S_a	surface of ship-a
T	draft
U	ship speed
x, y, z	coordinate system
x_b, y_b	position of ship-b
$\vec{W}$	steady flow velocity vector
β	wave direction

ζ_k^a	complex motion amplitude mode k of ship-a
λ	wavelength
λ_{jk}^{ab}	damping component j of ship-a for motion of ship-b in mode k
μ_{jk}^{ab}	added mass component j of ship-a for motion of ship-b in mode k
ν	radiation wavenumber
ρ	water density
σ_D^a	diffracted source strength on ship-a
σ_k^{ab}	source strength on ship-b due to mode k of ship-a
Φ	unsteady wave velocity potential
Φ_T	total velocity potential
ϕ_D	complex diffracted wave potential
ϕ_I	complex incident wave potential
ϕ_k^a	complex potential for mode k of ship-a
ϕ_R	complex radiated wave potential
ϕ_s	disturbed steady potential
ω	wave frequency
ω_e	wave encounter frequency
Δ_a	displacement of cylinder-a

INTRODUCTION

When two ships are advancing together at speed in close proximity in waves, the hydrodynamic forces on each ship are affected by shelter-

ing or wave-reflection from the neighbouring ship. This paper describes research that was initiated by the design process for a naval supply vessel, for which hydrodynamic interaction effects with receiving ships can be significant. The resulting computer program can predict added mass, wave radiation damping, and wave excitation forces acting on each vessel in the presence of the other.

The present code is an extension of a panel code by Huang and Hsiung [1] that was used by Howard, Calisal and Barnard [2] for computing hydrodynamic forces and resulting motions of a single ship in waves. The theory for incorporating interaction effects between two bodies has been developed by Van Oortmerssen [3], and Kokkinowrachos [4]. While codes for the single ship case utilize lateral symmetry, solution of the non-symmetrical two ship case using the current code requires approximately four times as many panels as for a single ship. Consequently, the computational requirements for memory and CPU time are of the order of sixteen times greater than for an individual ship case.

As a preliminary validation, computed forces are compared with published numerical and experimental results by Kokkinowrachos [4] for two vertical cylinders floating in waves with zero forward speed. To illustrate the influence of interaction effects on ship operations, predicted hydrodynamic forces are presented for a small vessel abeam of a large supply vessel.

FORMULATION

Figure 1 shows a plan view for solution of hydrodynamic interactions between two ships. The coordinate system has its origin in the calm water surface plane at midships of ship-a. The coordinates x_b, y_b represent the location of midships of ship-b. The incident wave direction β follows the convention of 180 degrees for head seas and 90 degrees for waves from starboard. The z axis has a positive-up direction.

Velocity Potentials

For oscillatory forces acting on a body in waves, viscous effects are small and it can be assumed that the fluid is inviscid and incompressible and that the flow is irrotational. The resultant velocity potential Φ_T in the vicinity of the ships can
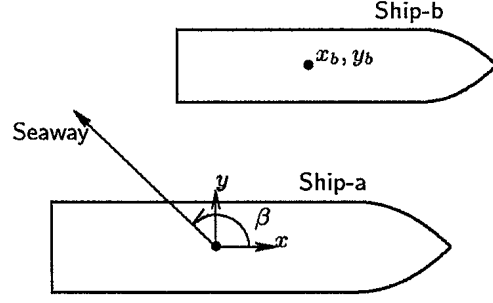

Figure 1: Plan View of Ship Interaction

be expressed as:

$$\Phi_T(x,y,z,t) = -Ux + \phi_s(x,y,z) + \Phi(x,y,z,t) \quad (1)$$

where U is steady forward speed of both ships, ϕ_s is the disturbed potential due to the presence of the ship in the steady incident flow, and Φ is the total oscillatory potential due to waves and ship motions. The term $-Ux$ represents the incident potential due to ship forward speed. The unsteady velocity potential Φ can be written as:

$$\Phi(x,y,z,t) = \text{Re}\left\{[\phi_I(x,y,z) + \phi_D(x,y,z) + \phi_R(x,y,z)]e^{-i\omega_e t}\right\} \quad (2)$$

where Re denotes the real part of the term in brackets, and ϕ_I, ϕ_D and ϕ_R are the complex values of the incident, diffracted, and radiated potentials, and ω_e is the wave encounter frequency.

Hydrodynamic Forces

The hydrodynamic forces acting on ship-a and ship-b can be expressed as:

$$F_j^a = \int_{S_a} p n_j^a dS \quad (j = 1, 2, ..., 6) \quad \text{on } S_a \quad (3)$$

$$F_j^b = \int_{S_b} p n_j^b dS \quad (j = 1, 2, ..., 6) \quad \text{on } S_b \quad (4)$$

where S_a and S_b are the wetted hull surfaces of ships a and b, and p is hydrodynamic pressure. The generalized unit normal of each ship can be expressed as shown here for ship-a.

$$n_j^a = \begin{cases} n_j^a & \text{for } j = 1, 2, 3 \\ \vec{r}_a \times \vec{n}_j^a & \text{for } j = 4, 5, 6 \end{cases} \quad (5)$$

where $\vec{r}_a$ is the moment arm vector from the origin to the point on the hull. For $j = 1, 2, 3$, n_j^a are the

components of the normal vector pointing into the hull of ship-a.

The hydrodynamic pressure p can be computed from:

$$p = -\rho \left(\frac{\partial \Phi}{\partial t} + \vec{W} \cdot \nabla \Phi \right) \qquad (6)$$

where ρ is water density. The steady flow velocity vector $\vec{W}$ is given by

$$\vec{W} = \nabla(-Ux + \phi_s) \qquad (7)$$

Substituting Equations (6) and (7) into Equations (3) and (4), the hydrodynamic force on the two ships can be expressed as:

$$F_j^a = \\ -\int_{S_a} \rho \left[\frac{\partial \Phi}{\partial t} + \nabla(-Ux + \phi_s) \cdot \nabla \Phi \right] n_j^a dS \qquad (8)$$

$$F_j^b = \\ -\int_{S_b} \rho \left[\frac{\partial \Phi}{\partial t} + \nabla(-Ux + \phi_s) \cdot \nabla \Phi \right] n_j^b dS \qquad (9)$$

By substituting the various components of Equation (2) into the above two equations, one can compute the incident wave force, diffracted wave force, or radiated wave forces acting on each ship.

RADIATION PROBLEM

The solution of hydrodynamic forces due to ship motions is called the radiation problem. For the present case of two ships in close proximity, the radiation solution must include interaction effects.

Radiation Potential

For two ships freely floating in calm water, the radiation wave velocity potentials can be determined by satisfying the body surface condition of two cases: 1) ship-a is in motion while ship-b is at rest; and 2) ship-b is in motion while ship-a is at rest.

The complex radiation potential from ships a and b, each having six degrees of freedom, can be expressed as:

$$\phi_R(x, y, z, t) = \sum_{k=1}^{6} \left[\zeta_k^a \phi_k^a + \zeta_k^b \phi_k^b \right] \qquad (10)$$

where ζ_k^a is the complex motion amplitude of ship-a for mode k, ϕ_k^a is the complex velocity potential for unit amplitude motions of ship-a while ship-b is at rest, and ζ_k^b and ϕ_k^b are corresponding values for ship-b.

The radiation velocity potentials ϕ_k^a and ϕ_k^b must satisfy several conditions. The solution of ϕ_k^a to satisfy these conditions will be presented here, with a similar solution existing for ϕ_k^b.

For potential flow, the radiation potential ϕ_k^a must satisfy Laplace's equation throughout the fluid:

$$\nabla^2 \phi_k^a = 0 \qquad (11)$$

The following boundary condition applies on the mean free surface:

$$\left(g\frac{\partial}{\partial z} + U^2 \frac{\partial^2}{\partial x^2} + 2i\omega_e U \frac{\partial}{\partial x} - \omega_e^2 \right) \phi_k^a \\ = 0 \quad \text{on } z = 0 \qquad (12)$$

The body normal boundary conditions on the moving ship-a, the stationary ship-b, and ocean bottom are:

$$\frac{\partial \phi_k^a}{\partial n} = n_k^a - \frac{m_k^a}{i\omega_e} \quad \text{on } S_a \qquad (13)$$

$$\frac{\partial \phi_k^a}{\partial n} = 0 \quad \text{on } S_b \qquad (14)$$

$$\frac{\partial \phi_k^a}{\partial z} = 0 \quad \text{on } z = -\infty \qquad (15)$$

where m_k^a is the generalized body normal vector including the effect of ship forward speed, as described in Reference 1. The velocity potential ϕ_k^a must also satisfy the condition that waves radiate outward from the body.

The solution of the velocity potential ϕ_k^a is facilitated by a Green function that satisfies all boundary conditions except the body boundary conditions of Equations 13 and 14. These boundary conditions can be satisfied by placing sources of strength σ_k^{aa} on ship-a and strength σ_k^{ab} on ship-b. The radiation potentials due to motions of ship-a while ship-b is stationary can then be expressed as:

$$\phi_k^a(p) = \int_{S_a} \sigma_k^{aa}(q) G(p; q) dS(q) \\ + \int_{S_b} \sigma_k^{ab}(q) G(p; q) dS(q) \qquad (16)$$

where p is the location of a point in the fluid domain, $G(p; q)$ is the Green function, and q is the location of a point on the hull surface. The Green function satisfying the continuity equation

3

and most of the boundary conditions is:

$$G(p;q) = \frac{1}{r_1} + \frac{1}{r_2} + 2\nu \int_0^\infty \frac{e^{k(z_p+z_q)}}{k-\nu} J_0(\nu R)dk$$
$$+i2\pi\nu e^{\nu(z_p+z_q)} J_0(\nu R) \qquad (17)$$

where x_p, y_p, z_p are the coordinates of point p, x_q, y_q, z_q are the coordinates of point q, $\nu = \omega_e^2/g$ is the radiation wavenumber, and J_0 is the Bessel function of the first kind of order zero. The terms r_1 and r_2 denote the distance from a field point to a source and to its image, respectively, and are given by:

$$r_1 = \sqrt{(x_p-x_q)^2 + (y_p-y_q)^2 + (z_p-z_q)^2} \quad (18)$$
$$r_2 = \sqrt{(x_p-x_q)^2 + (y_p-y_q)^2 + (z_p+z_q)^2} \quad (19)$$

The term R is the horizontal distance between the field and source points:

$$R = \sqrt{(x_p-x_q)^2 + (y_p-y_q)^2} \qquad (20)$$

Applying the hull body boundary conditions of Equations 13 and 14, the source strengths σ_k^{aa} and σ_k^{ab} due to motions of ship-a for each mode k are solved by satisfying the following equations simultaneously:

$$\int_{S_a} \sigma_k^{aa}(q) \frac{\partial G(p;q)}{\partial n} dS(q)$$
$$+ \int_{S_b} \sigma_k^{ab}(q) \frac{\partial G(p;q)}{\partial n} dS(q)$$
$$= n_k^a - \frac{m_k^a}{i\omega_e} \quad \text{on } S_a \qquad (21)$$
$$\int_{S_a} \sigma_k^{aa}(q) \frac{\partial G(p;q)}{\partial n} dS(q)$$
$$+ \int_{S_b} \sigma_k^{ab}(q) \frac{\partial G(p;q)}{\partial n} dS(q)$$
$$= 0 \quad \text{on } S_b \qquad (22)$$

Once the complex source densities σ_k^{aa} and σ_k^{ab} are solved, the complex radiation velocity potentials ϕ_k^a can be determined using Equation (16). For radiation due to motions of ship-b while ship-a is stationary, the source densities σ_k^{ba} and σ_k^{bb} and potentials ϕ_k^b can be solved in a similar manner.

Added Mass and Damping

Once the radiation potentials are known, the added mass and damping terms can be evaluated.

The radiation force component j acting on ship-a can be expressed as:

$$F_j^{Ra}(x,y,z,t) =$$
$$\sum_{k=1}^{6} \left[-\ddot{\zeta}_k^a \mu_{jk}^{aa} - \dot{\zeta}_k^a \lambda_{jk}^{aa} - \ddot{\zeta}_k^b \mu_{jk}^{ab} - \dot{\zeta}_k^b \lambda_{jk}^{ab} \right] \quad (23)$$

where μ_{jk}^{aa} is added mass due to motion component k of ship-a, λ_{jk}^{aa} is damping due to motion component k of ship-a, μ_{jk}^{ab} is added mass due to motion component k of ship-b, and λ_{jk}^{ab} is damping due to motion component k of ship-b. Based on Equations (8), (10), and (23), the added mass and damping coefficients for forces on ship-a are:

$$\mu_{jk}^{aa} = \rho \left\{ \int_{S_a} \text{Re}[\phi_k^a] n_j^a dS \right.$$
$$+ \frac{U}{\omega_e} \int_{S_a} \text{Im}\left[\frac{\partial \phi_k^a}{\partial x}\right] n_j^a dS$$
$$\left. - \frac{1}{\omega_e} \int_{S_a} \text{Im}\left[\nabla \phi_k^a \cdot \nabla \phi_s\right] n_j^a dS \right\} \quad (24)$$

$$\mu_{jk}^{ab} = \rho \left\{ \int_{S_a} \text{Re}[\phi_k^b] n_j dS \right.$$
$$+ \frac{U}{\omega_e} \int_{S_a} \text{Im}\left[\frac{\partial \phi_k^b}{\partial x}\right] n_j^a dS$$
$$\left. - \frac{1}{\omega_e} \int_{S_a} \text{Im}\left[\nabla \phi_k^b \cdot \nabla \phi_s\right] n_j^a dS \right\} \quad (25)$$

$$\lambda_{jk}^{aa} = \rho \left\{ \omega_e \int_{S_a} \text{Im}[\phi_k^a] n_j^a dS \right.$$
$$- U \int_{S_a} \text{Re}\left[\frac{\partial \phi_k^a}{\partial x}\right] n_j^a dS$$
$$\left. + \int_{S_a} \text{Re}\left[\nabla \phi_k^a \cdot \nabla \phi_s\right] n_j^a dS \right\} \quad (26)$$

$$\lambda_{jk}^{ab} = \rho \left\{ \omega_e \int_{S_a} \text{Im}\left[\phi_k^b\right] n_j^a dS \right.$$
$$- U \int_{S_a} \text{Re}\left[\frac{\partial \phi_k^b}{\partial x}\right] n_j^a dS$$
$$\left. + \int_{S_a} \text{Re}\left[\nabla \phi_k^b \cdot \nabla \phi_s\right] n_j^a dS \right\} \quad (27)$$

The added mass and damping coefficients for forces on ship-b are evaluated in a similar manner.

WAVE EXCITATION FORCE

The wave excitation force on a ship-a in regular waves can be expressed in terms of complex forces due to incident and diffracted waves:

$$F_j^{Wa}(t) = \text{Re}\left[(f_j^{Ia} + f_j^{Da})e^{-i\omega_e t}\right] \quad (28)$$

4

where f_j^{Ia} is the complex incident (Froude-Krylov) force and f_j^{Da} is the diffracted wave force.

Incident Wave Force

The complex incident wave potential introduced in Equation (2) is the following for unit amplitude waves:

$$\phi_I = \frac{g}{i\omega} \cdot e^{kz + ik(x\cos\beta + y\sin\beta)} \qquad (29)$$

where g is acceleration due to gravity and β is the wave direction relative to the ship heading (see Figure 1). The wavenumber k of the incident waves is given by:

$$k = \frac{\omega^2}{g} \qquad (30)$$

The relationship between the wave encounter frequency and wave frequency is:

$$\omega_e = \omega - kU\cos\beta \qquad (31)$$

Substituting the complex incident wave potential ϕ_I into equation (8), the complex incident wave excitation force is:

$$
\begin{aligned}
f_j^{Ia} = &-\rho\omega \int_{S_a} Im\,[\phi_I]\,n_j^a dS \\
&-\rho \int_{S_a} \mathrm{Re}\,[\nabla\phi_I \cdot \nabla\phi_s]\,n_j^a dS \\
&+i\left\{ \rho\omega \int_{S_a} \mathrm{Re}\,[\phi_I]\,n_j^a dS \right. \\
&\left. -\rho \int_{S_a} Im\,[\nabla\phi_I \cdot \nabla\phi_s]\,n_j^a dS \right\} \qquad (32)
\end{aligned}
$$

The above equation utilizes the relationship between wave frequency and wave encounter frequency of Equation (31) to include the speed dependent terms of Equation (8). The excitation force on ship-b is found in a similar manner.

Diffracted Wave Force

The presence of the two ships in waves will modify the incident wave field, creating a diffracted wave force on each ship. The diffracted wave forces are solved using a source distribution method similar to that used for the radiation forces; however, the diffracted wave potential only needs to be solved for the case of two stationary ships in waves. The resulting boundary conditions on the ship hulls for the complex diffracted potential ϕ_D are:

$$\frac{\partial\phi_D}{\partial n} = -\frac{\partial\phi_I}{\partial n} \qquad \text{on } S_a \qquad (33)$$

$$\frac{\partial\phi_D}{\partial n} = -\frac{\partial\phi_I}{\partial n} \qquad \text{on } S_b \qquad (34)$$

The diffracted potential is represented by a series of sources on both ships:

$$
\begin{aligned}
\phi_D(p) = &\int_{S_a} \sigma_D^a(q) G(p;q) dS(q) \\
&+ \int_{S_b} \sigma_D^b(q) G(p;q) dS(q) \qquad (35)
\end{aligned}
$$

where $\sigma_D^a(q)$ is the source density on ship-a and $\sigma_D^b(q)$ is the source density on ship-b. The Green function $G(p;q)$ of equation (17) again satisfies all conditions except the ship hull boundary conditions. Applying the body surface boundary conditions, the diffracted source strengths are solved to satisfy the following equations simultaneously:

$$
\begin{aligned}
&\int_{S_a} \sigma_D^a(q)\frac{\partial G(p;q)}{\partial n} dS(q) \\
&+ \int_{S_b} \sigma_D^b(q)\frac{\partial G(p;q)}{\partial n} dS(q) = -\frac{\partial\phi_I}{\partial n} \quad \text{on } S_a \; (36)
\end{aligned}
$$

$$
\begin{aligned}
&\int_{S_a} \sigma_D^a(q)\frac{\partial G(p;q)}{\partial n} dS(q) \\
&+ \int_{S_b} \sigma_D^b(q)\frac{\partial G(p;q)}{\partial n} dS(q) = -\frac{\partial\phi_I}{\partial n} \quad \text{on } S_b \; (37)
\end{aligned}
$$

After solving the diffracted source strengths, the diffracted potentials are then computed using equation (35). These diffracted potentials can then be substituted into equation (8) to get the diffracted wave force on ship-a:

$$
\begin{aligned}
f_j^{Da} = &-\rho\omega_e \int_{S_a} Im\,[\phi_D]\,n_j^a dS \\
&+\rho U \int_{S_a} \mathrm{Re}\left[\frac{\partial\phi_D}{\partial x}\right] \\
&-\rho \int_{S_a} \mathrm{Re}\,[\nabla\phi_D \cdot \nabla\phi_s]\,n_j^a dS \\
&+i\left\{ \rho\omega_e \int_{S_a} \mathrm{Re}\,[\phi_D]\,n_j^a dS \right. \\
&+\rho U \int_{S_a} Im\left[\frac{\partial\phi_D}{\partial x}\right] \\
&\left. -\rho \int_{S_a} Im\,[\nabla\phi_D \cdot \nabla\phi_s]\,n_j^a dS \right\} \qquad (38)
\end{aligned}
$$

The diffracted forces on ship-b are solved in a similar manner.

COMPUTATIONS FOR TWO CIRCULAR CYLINDERS

The computer program was initially validated using results from References 3 and 4. Figure 2 presents the case of two stationary vertical circular cylinders floating in waves, which was used for comparison with computations by Kokkinowrachos [4]. Each cylinder has radius r and draft equal to $1/2$ r. The computations presented here are for a separation distance between vertical axes of $5r$. The wave direction is along the x axis, which passes through both cylinders. For the present discussion, the cylinder on the left is referred to as exposed cylinder-a, while the cylinder on the right is referred to as sheltered cylinder-b. Each cylinder has 92 panels for computations.
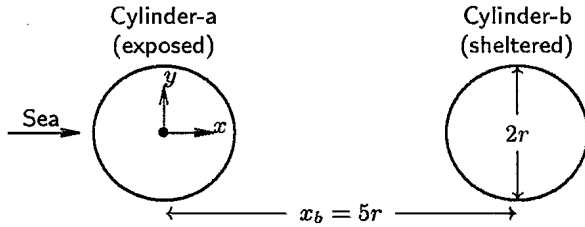
Figure 2: Two Identical Circular Cylinders Floating in Waves

Figures 3 to 8 show sample computed results for the two cylinder case of Figure 2 and for a single cylinder. Agreement with computations by Kokkinowrachos for two cylinders is very good, suggesting that the method has been correctly implemented. Figures 3 and 4 indicate that the surge excitation force on the exposed cylinder is influenced significantly by the sheltered cylinder; however, the influence on the sheltered cylinder is small. For heave excitation, interaction effects have only a small influence on both cylinders. The heave interaction added mass and damping terms shown in Figures 7 and 8 appear to be significant. Because the two cylinders have identical dimensions, the interaction terms μ_{ij}^{ab} and λ_{ij}^{ab} are equal to μ_{ij}^{ba} and λ_{ij}^{ba} for all values of i and j.

WAVE EXCITATION FORCES ON TWO SHIPS

After successful validation, the program was run for a naval Maritime Coastal Defence Vessel (MCDV) abeam of a supply vessel (AOR), with
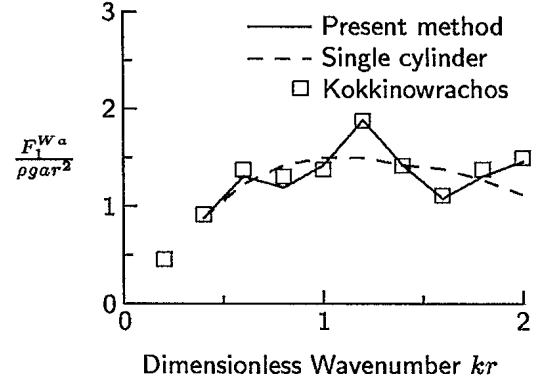
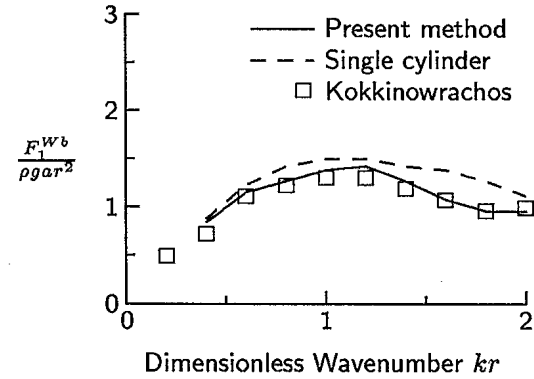Figure 3: Surge Excitation on Exposed Cylinder-a

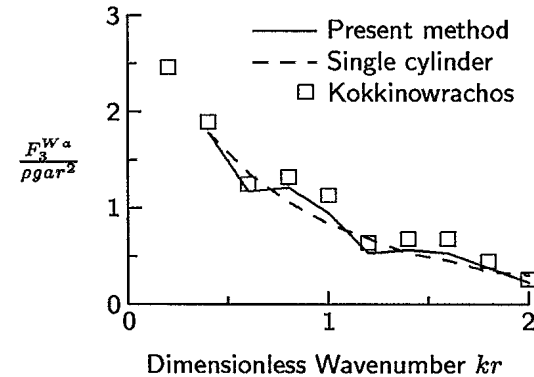Figure 4: Surge Excitation on Sheltered Cylinder-b

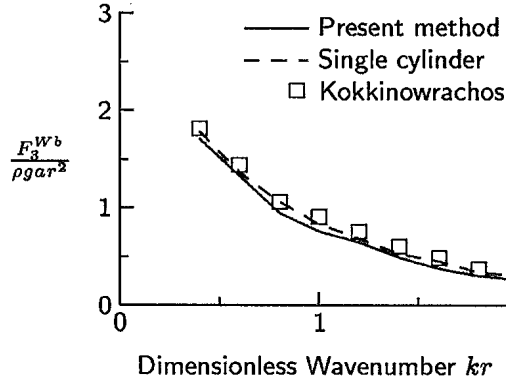
Figure 5: Heave Excitation on Exposed Cylinder-a

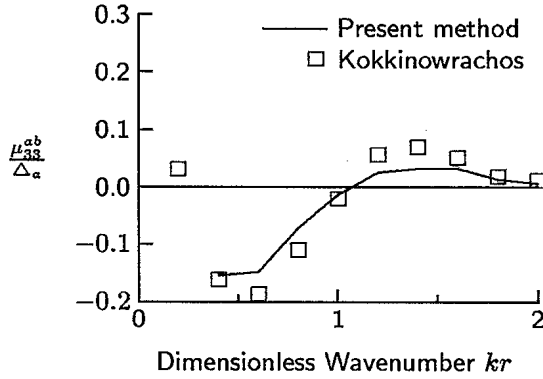Figure 6: Heave Excitation on Sheltered Cylinder-b

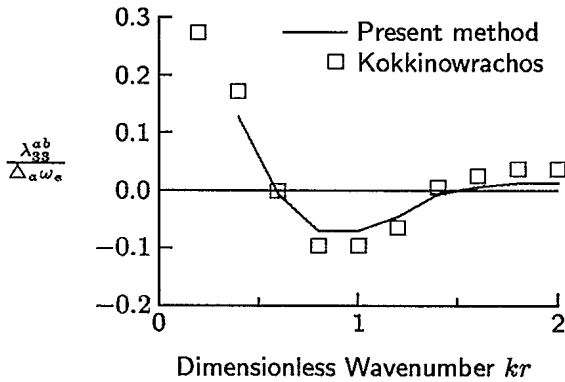Figure 7: Heave Added Mass Interaction for Cylinders

Figure 8: Heave Damping Interaction for Cylinders

both ships travelling at 10 knots. Table 1 gives dimensions for both ships. Using the notation of Figure 1, the AOR is ship-a and the smaller MCDV is ship-b. For the present computations, midships of the MCDV is aligned longitudinally with midships of the AOR (i.e. $x_b = 0$). Lateral offsets of 25.44 m and 500 m for the MCDV are used, giving a narrow gap of 8.5 m between ships for the first case and a very wide separation distance for the second case.

Each ship is panelled with approximately 20 panels longitudinally by 10 panels girthwise, resulting in 200 panels for the AOR and 212 panels for the MCDV. The maximum nominal panel dimension is approximately 8 m, representing the longitudinal dimension of panels on the AOR hull. According to Sarpkaya and Isaacson [5], a panel method should be able to give accurate results for wavelengths greater than 8 times the maximum panel dimension; thus, the current panelling scheme should give good results for wavelengths greater than 64 m, representing $\lambda/L_b > 1.2$. The panel size should also be less than the gap between two bodies in close proximity, which is satisfied for the current cases.

Table 1: Dimensions of AOR and MCDV

	AOR	MCDV
Length, L	162.5 m	52.0 m
Beam, B	23.16 m	10.76 m
Draft, T	9.14 m	3.4 m
Block coefficient, C_B	0.60	0.56

Beam Seas

Figures 9 to 16 give sway and heave excitation forces acting on the MCDV and AOR from the two possible beam seas directions. Wave length λ is non-dimensionalized by the MCDV length L_b for all figures. For each combination of ship speed, wave heading, separation configuration, and wavelength, the computation time was approximately one hour on a workstation with speed ratings of 85 MIPS and 70 SPECmarks, leading to a computation time of approximately 60 hours for the two headings, two separation distances, and 15 wavelengths presented here.

Figures 9 and 10 show that the sway excitation on the MCDV is dramatically reduced when it is sheltered by the AOR. The sheltering effect is

7

surprisingly great at the large separation distance of 500 m. As expected, Figures 11 and 12 show that the MCDV has very little influence on the AOR sway excitation. Figures 13 and 14 indicate that interaction effects on the MCDV are significant for heave excitation but less dramatic than for sway excitation. The heave excitation on the AOR shown in Figures 15 and 16 varies little with proximity to the MCDV.
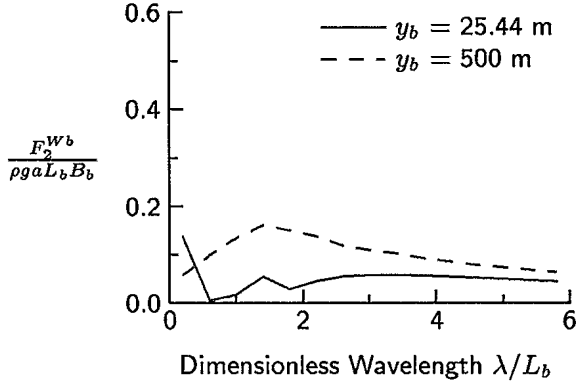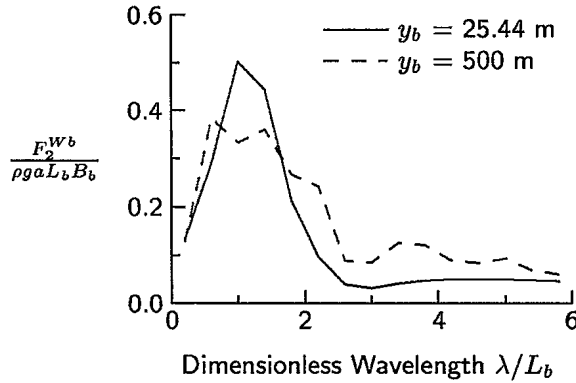

Figure 9: Sway Excitation on MCDV Abeam of AOR, $\beta = 90$ degrees (MCDV Sheltered)

Figure 10: Sway Excitation on MCDV Abeam of AOR, $\beta = 270$ degrees (MCDV Exposed)

Head Seas

Because ships typically head into waves during replenishment-at-sea operations, additional computations were performed for the MCDV abeam of the AOR in head seas at a speed of 10 knots. Figures 17 to 20 show heave and pitch excitation forces on the MCDV and AOR. With the exception of heave excitation on the MCDV in the vicinity of $\lambda/L_b = 2$, interaction effects are very small. The
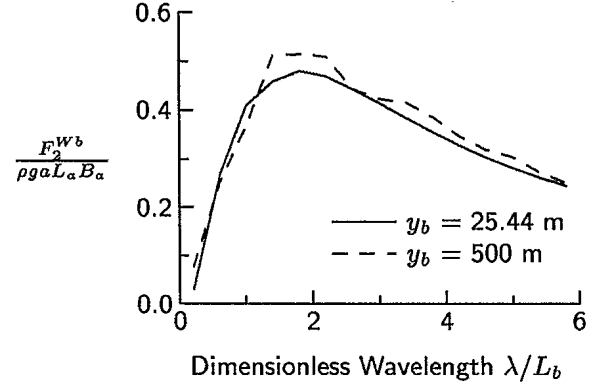
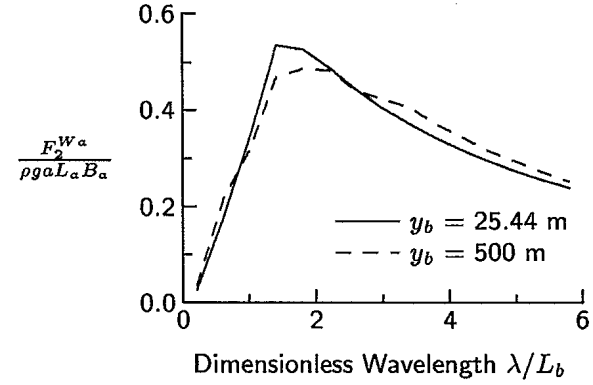Figure 11: Sway Excitation on AOR Abeam of MCDV, $\beta = 90$ degrees (AOR Exposed)

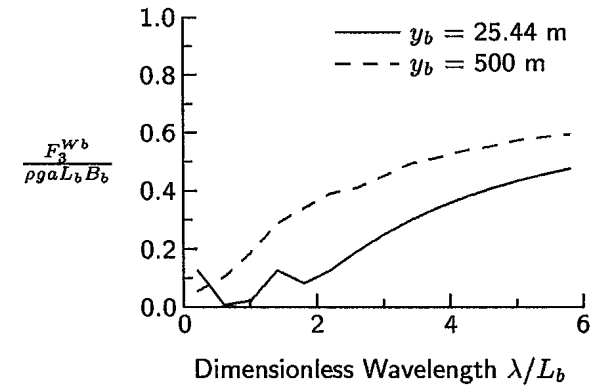Figure 12: Sway Excitation on AOR Abeam of MCDV, $\beta = 270$ degrees (AOR Sheltered)

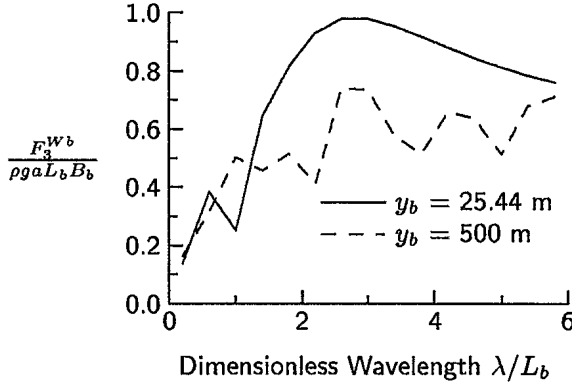Figure 13: Heave Excitation on MCDV Abeam of AOR, $\beta = 90$ degrees (MCDV Sheltered)

8

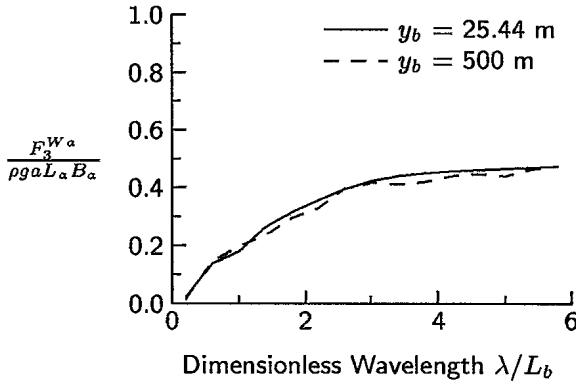Figure 14: Heave Excitation on MCDV Abeam of AOR, $\beta = 270$ degrees (MCDV Exposed)

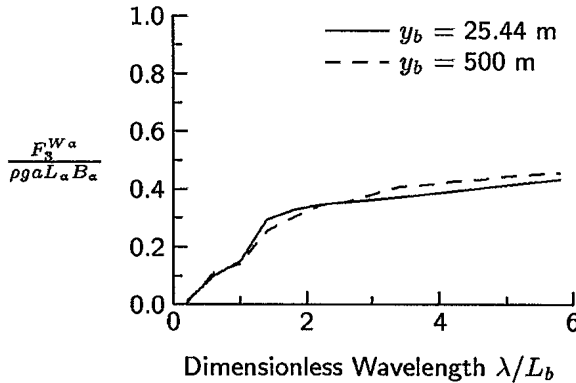Figure 15: Heave Excitation on AOR Abeam of MCDV, $\beta = 90$ degrees (AOR Exposed)

Figure 16: Heave Excitation on AOR Abeam of MCDV, $\beta = 270$ degrees (AOR Sheltered)

large increase in heave excitation for the MCDV could be due to either wave resonance between the two vessels or to numerical problems caused by the narrow gap between the vessels.
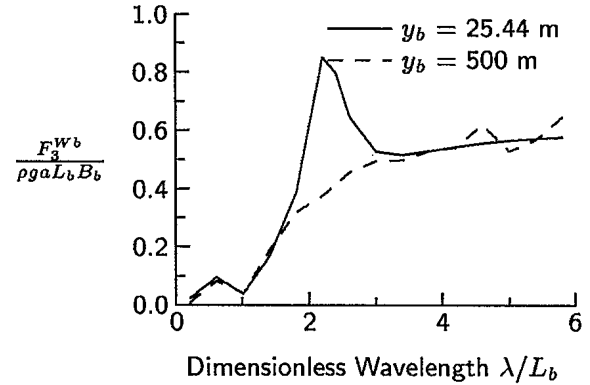

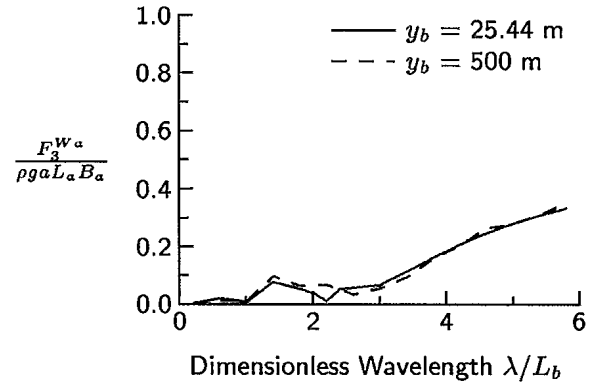Figure 17: Heave Excitation on MCDV Abeam of AOR, Head Seas

Figure 18: Heave Excitation on AOR Abeam of MCDV, Head Seas

CONCLUSIONS

A computer program has been developed for computing the unsteady hydrodynamic forces on two ships in close proximity. The aim of the program was to investigate interaction effects during operations such as replenishment-at-sea.

The mathematical solution satisfies boundary conditions on both ship hulls simultaneously for the radiation and diffraction potentials. The lack of lateral symmetry for the two ship case causes the number of panels to be approximately 4 times greater and the computational effort to be approximately 16 times greater than for a single ship.
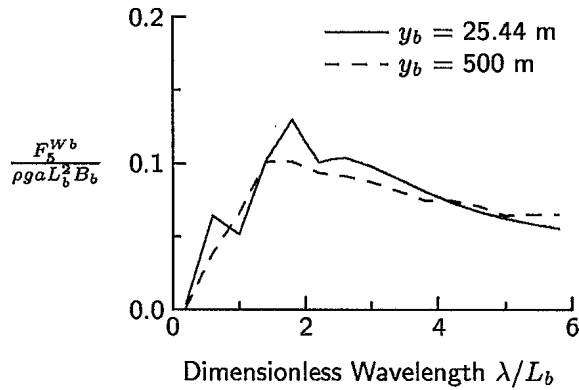
9

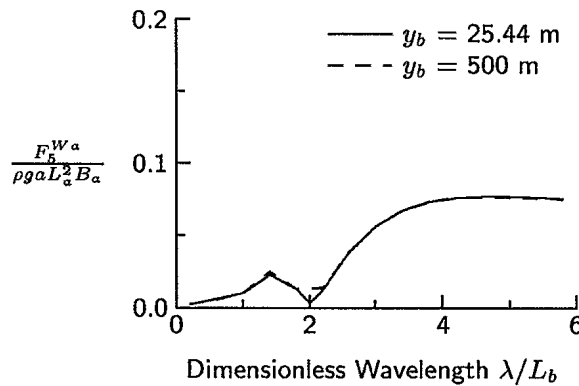Figure 19: Pitch Excitation on MCDV Abeam of AOR, Head Seas

Comparisons with published results for hydrodynamic forces on two circular cylinders indicate that the computer program is giving correct results. Computations for a Maritime Coastal Defence Vessel operating abeam a supply ship show that interaction effects are very significant for excitation forces in beam seas but are small in head seas, with the exception of a narrow wavelength range for which a resonance phenomenon appears to occur.

The present computer program has potential to assist with design and planning for replenshment-at-sea; however, the program should first be validated with experimental data for two ships in close proximity. Given a lack of experimental data, a new series of wave tank experiments would likely be required for program validation.

REFERENCES

[1] Z.J. Huang and C.C. Hsiung, "An Improved 3-D Panel Method to Compute mj-Terms for Ship Motion," in *Proceedings of the Second Canadian Marine Dynamics Conference* (Vancouver, August 1993), pp. 50–56.

[2] J.D. Howard, S.M. Calisal, and L. Barnard, "Seakeeping Evaluation of a Low L/B Hull Form Series," in *Proceedings of the Third Canadian Marine Hydrodynamics and Structures Conference* (Dartmouth, Nova Scotia, August 1995), pp. 125–135.

[3] G. van Oortmerssen, "Hydrodynamic Interaction Between Two Structures Floating in Waves," in *Second International Conference on Behaviour of Off-Shore Structures, BOSS'79* (London, August 1979).

[4] K. Kokkinowrachos, "Hydrodynamic Interaction between Several Vertical Bodies of Revolution in Waves," in *Fifth International Symposium on Offshore Mechanics and Arctic Engineering (OMAE)* (Tokyo, 1986), Vol. 1.

[5] T. Sarpkaya and M. Isaacson, *Mechanics of Wave Forces on Offshore Structures*, Van Nostrand Reinhold, 1981.

Figure 20: Pitch Excitation on AOR Abeam of MCDV, Head Seas

10

#503453